CHITOSAN-BASED FILMS WITH SILVER NANOPARTICLES PREPARED USING METAL VAPOR SYNTHESIS

Margarita S. Rubina*, Alexander V. Naumkin, Alexander Yu. Vasilkov

A. N. Nesmeyanov Institute of Organoelement Compounds of Russian Academy of Sciences, Vavilova str. 28, 119991 Moscow, Russia

Abstract

In this work a novel route to obtain chitosan-based films with silver nanoparticles is presented. Silver nanoparticles were synthesized via sustainable metal-vapor synthesis and then deposited on chitosan powder. Films were prepared with a casting method from polymer solution containing silver nanoparticles in acetic acid. X-ray photoelectron spectroscopy was used to evaluate a chemical composition, relative concentration of functional groups and charge state of metal atoms on the surface of materials. Structure and possible stabilization mechanisms of metal nanoparticles in polymer matrix were studied using Fourier-transform infrared spectroscopy in the attenuated total reflectance mode. The prepared films have potential to be used as dressing materials in regenerative medicine for treatment of wounds and burns.

Key words: *chitosan, silver nanoparticles, metal vapor synthesis, XPS, ATR-FTIR, chitosan films*

1. INTRODUCTION

Chitosan is a linear polysaccharide of cationic nature consisting from D-glucosamine and N-acetyl-D-glucosamine units. This polymer possesses unique properties such as biodegradability, biocompatibility, non-toxicity as well as antimicrobial activity and can be used different fields such as medicine, agriculture etc [1]. Chitosan also has good film-forming properties beneficial for producing films and coating materials. Chitosan-based films as food packaging materials are used in the food and agriculture industry [2, 3]. It is known that chitosan promotes the dermal regeneration during skin reconstruction through various mechanisms. Thus chitosan-based films could be successfully applied in treatments of burns and wounds [4]. Introduction of silver nanoparticles into chitosan films enhances antimicrobial properties of the material due to the known bactericidal activity of the nanoparticle against a broad spectrum of bacteria, including antibiotic resistant [5].

The most common way to produce silver nanoparticles is chemical reduction method in which one of the special additives such as sodium borohydride, sodium citrate or sodium ascorbate are used [6]. Also, the reduction of metal ions through UV, microwave and sound irradiation can be performed. As a reducing agent and stabilizer for nanoparticles chitosan molecules can be effectively used [7,8]. However, some difficulties are associated with using these methods, mainly concerning the level of metal reduction control and the necessity to deal with by-products.

One of the effective methods of obtaining nanocomposites for biomedical applications is metal vapor synthesis (MVS) [9-11]. This method is sustainable and no by-products are formed during the metal containing composites synthesis. We have previously demonstrated that MVS can be used to obtain chitosan-based powders with gold, iron, copper and zinc nanoparticles and reported the structure of the composites [12-14]. Copper and zinc containing composites were proven to be effective against pathogenic necrotrophic microorganisms *Sclerotium rolfsii* and *Rhizoctonia solani* that cause a wide range of commercially significant plant diseases [13, 14].

In this paper a novel method for preparing chitosan-based films doped with silver nanoparticles is proposed. The surface composition of the films was studied by means of XPS. ATR-FTIR technique was used to identify specific interactions between functional groups of chitosan chains and surface of nanoparticles.

2. EXPERIMENTAL PART

2.1. Materials

Chitosan with low molecular weight was purchased from Sigma Aldrich (#448869) and was used without any additional purification procedure. Isopropyl alcohol (Panreac, HPLC-grade) was used as a solvent in MVS. Prior to synthesis solvent was dried under molecular sieves (4 Å) and degassed at a residual pressure of 10^{-1} Pa by freezing-thawing cycles. Silver with 99.99% purity was used in the form of foils. For films preparation glacial acetic acid and sodium hydroxide of analytical grade were used. To prepare solutions deionized water Mili-Q (18 MΩ) was used.

2.2. Preparation of chitosan doped with Ag nanoparticles using metal vapor synthesis

The metal vapor synthesis was used for the preparation of colloidal solution of silver nanoparticles. Then the solution was deposited on chitosan powder. Detailed information about typical MVS procedure was reported previously [13]. Briefly, silver foil with mass of 420 mg (3.7 mmol) was evaporated from Ta-boat under vacuum of 10^{-3} Pa and condensed with ca. 120 ml (1.6 mol) of isopropyl alcohol on liquid N_2-cooled walls of a reactor. In a typical experiment the molar metal to solvent ratio was ca. 1:430. Mass of chitosan powder for deposition was 4.0 g.

2.3. Preparation of chitosan films doped with Ag nanoparticles

Chitosan powder containing silver nanoparticles (2 wt%) was dissolved in glacial acetic acid solution (1 v/v%) in Mili-Q water during vigorous stirring at RT until a homogenous solution was obtained. Films were obtained through casting method. For this purpose chitosan solution was poured onto glass surface of Petri dish with diameter of 9 cm. Then films were air-dried during 48 hours under RT and relative humidity ca. 50 %. After that, the films were immersed in a 1M solution of sodium hydroxide during 1 hour, followed by washing in deionized water to achieve neutral pH, and dried at RT to constant mass. The films were prepared from pristine chitosan powder (ChitFilm) as well as from chitosan modified with silver nanoparticles (Ag/ChitFilm).The air-dried films were stored in tightly closed zip-bags. Thick chitosan-based films with thickness of 70 μm were used for XPS and ATR-FTIR analysis.

2.4. Characterization methods

Concentration of silver was measured with VRA 30 X-Ray fluorescent analyzer (Germany) using the Ag Kα line of X-Ray fluorescence spectrum. In order to excite radiation, X-ray tube with a Mo anode was used at a mode of 50 kV and 20 μA. Thickness of casting films was determined with digital micrometer. The average value of thickness was obtained with 5 measurements in different areas of films. TEM images were performed using a transmission electron microscope LEO 912AB OMEGA, Zeiss (Germany) at acceleration voltage of 100 kV. Micrographs were analyzed using ImageJ and OriginPro8 software. FT-IR spectra were collected using Thermo Nicolet Nexus spectrometer equipped with ATR attachment at 2 cm^{-1} resolution in the region from 4000 to 400 cm^{-1}. For ATR-FTIR measurements ZnSe crystal was used. Before measurements the films were stored at RT in plastic zip-bags. X-ray photoelectron spectra were acquired with a ThermoFisher Scientific Theta Probe spectrometer using monochromatized Al Kα radiation (1486.6 eV) at an operating power of 150 W of the X-ray tube with a step size of 0.1 eV. Sample charging was corrected by referencing to the C-C/C-H peak deconvoluted in the C 1s spectrum (284.8 eV).

3. RESULTS AND DISCUSSION

MVS method for preparation of colloidal solution of metal nanoparticles was carried out using previously developed procedure. The prepared colloidal solution of silver nanoparticles in isopropyl alcohol was used to modify chitosan powder and obtain Ag/Chit composite. Metal to solvent molar ratio was adjusted in order to minimize nanoparticles aggregation.

3.1. TEM analysis

Silver content (w/w) in biopolymer matrix after deposition procedure determined with X-ray fluorescence analysis was 1.2 %. TEM images in bright field and selected area diffraction pattern (SAED) for prepared Ag/Chit composite are shown in Fig. 1. The measured nanoparticles sizes were in the range of 3.6<d<12.1 nm with an average particle size of 6.3±2.0 nm. During the calculation the agglomerates of primary particles were not taken into account. The SAED pattern contains four bright rings with reflexes attributed to (111), (200), (220) and (311) crystallographic planes of metallic silver.

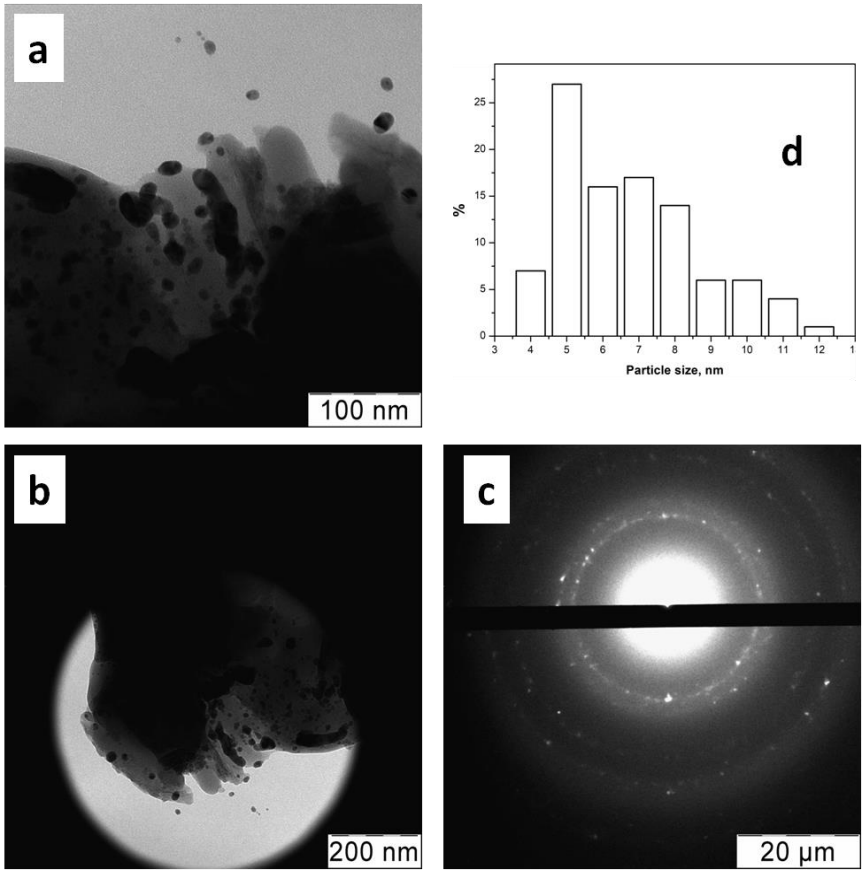

Fig. 1. TEM images in bright (a, b) and dark fields (c) of Ag/Chit composite as well as SAED pattern (d) of highlighted field.

In order to produce the films, the method of casting from polymer solutions was used. It is well known that chitosan is nonsoluble in aqua or organic solvents but it is soluble in acidic aqueous solutions when pH of solution is near pKa of the glucosamine unit. The thickness of ChitFilm and Ag/ChitFilm measured using digital micrometer was 70 µm. The silver content calculated from elemental analysis data was 4.2 mg per 320 mg of biopolymer.

3.2. ATR-FTIR analysis

FTIR spectra of pristine chitosan film and film with silver nanoparticles recorded with ATR technique are shown in the Fig.2. Before analysis spectra were normalized at the reference peak of 2869 cm^{-1}. All spectra peaks are broadened and consist of overlapping bands which complicates peak analysis. Bce Second derivative spectroscopy method was used in this work in order to enhance the separation of overlapping peaks [15, 16]. Using this approach for 1400-800 cm^{-1} spectra regions exact peak wavenumbers were determined. Both spectra contain bands at 1409 and 1378 cm^{-1} attributed to the bending vibrations of methylene and methyl groups (in amide), respectively. Wide bands at 1338-1308

cm^{-1} and 1253 cm^{-1} correspond to CH_2 wagging vibration in primary alcohol, and the amide III vibration comes from a combination of N-H deformation and C-N stretching, respectively [17]. Intense band at 1152 cm^{-1} is related to asymmetric stretching vibrations in oxygen C-O-C bridge (glicosidic linkage) [15]. Peaks at 1126, 1098, 1068, 1019 cm^{-1} can also be identified and attributed to skeletal stretching vibrations in C-O containing groups (glicosodic linkage, primary alcohol). Broad region at ca. 3670-2380 cm^{-1} contains overlapping absorption N-H and O-H peaks (ca. 3500-3200 cm^{-1}) as well as of asymmetric (ca. 2915 cm^{-1}) and symmetric (ca. 2869 cm^{-1}) C-H stretching vibrations.

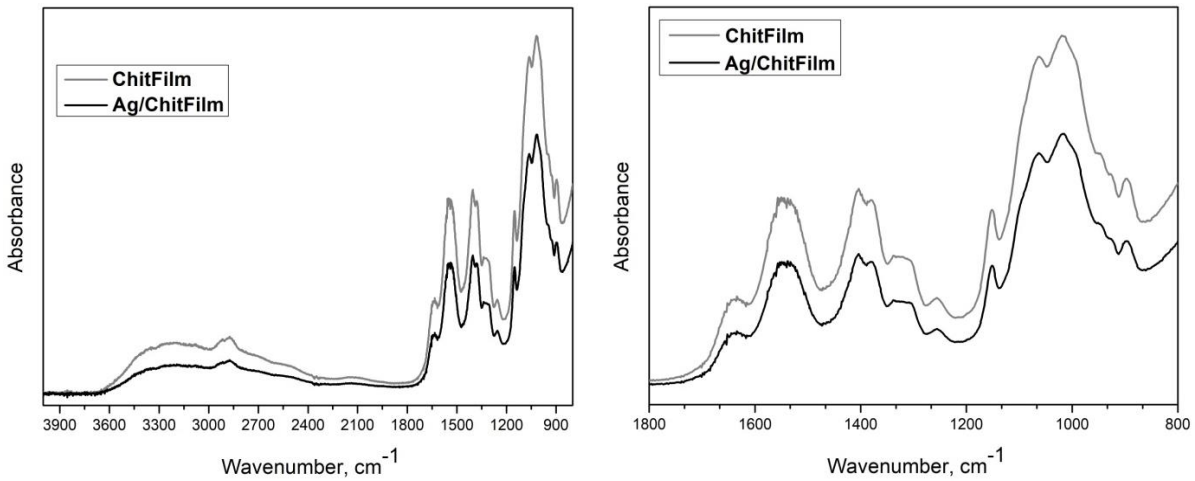

Fig. 2. ATR-FTIR spectra for the chitosan-based films in wide and narrow regions.

Particular attention should be paid to the broad bands positioned at ca. 1639 and ca.1540 cm^{-1}, the so-called amide I and amide II regions, respectively. To identify possible differences in the spectra of chitosan-based films a fitting procedure in amide region was performed. The shape of peaks was assumed to be Gaussian. The curve fitting was performed with OriginPro8 software. As a result, three peaks were isolated and attributed to amide I, amide II and N-H bending vibrations (Table 1). As it can be seen the wavenumbers are practically identical whereas the relative intensities are different. It can be assumed that the changes in relative peak intensities may arise from redistribution of electron density in polymer induced with the silver nanoparticles. Thus, surface of nanoparticles can interact with chitosan molecules due to electrostatic interactions where silver particles act as an acceptor and chitosan groups are donors [7, 16].

Table 1. Results of the spectra fitting in the amide I and amide II regions

Sample	Wavenumbers, cm^{-1}	FWHH	Area, %
ChitFilm	1641	46.28	2.441
	1555	52.16	6.363
	1518	36.84	1.942
Ag/ChitFilm	1641	44.88	1.454
	1553	53.27	4.512
	1517	33.28	1.082

In summary, spectra of both films have rather similar appearance, namely, there is neither changing in the band shapes or shifts to higher/lower wavenumbers. However, the significant decrease in

absorbance of all bands is detected. This indicates the attachment of silver nanoparticles to chitosan groups, which was previously proposed. Nevertheless, it is worth emphasizing that the difference in absorbance may also arise with changes in crystallinity of the films and polymer content. FTIR spectroscopy revealed no pronounced changes in the spectrum of the chitosan film under the influence of silver nanoparticles, which can be explained by a rather low concentration of metal in the sample. In order to more accurately detect certain types of interactions further investigations are required.

3.3. XPS analysis

Survey photoelectron spectra of Ag/ChitFilm and ChitFilm contain not only the characteristic peaks for biopolymer (C, N, O) but the peaks corresponding to Ca, Na, Si atoms as well, whereas for Ag/Chit composite the additive elements are not detected (Fig. 3). The appearance of these atoms in the surface layers of the samples can be explained by the preparation procedure of films (dissolution in acetic acid, exposure of the films in alkali solution and washing with deionized water). The quantification data based on the atomic sensitivity factors are given in Table 2.

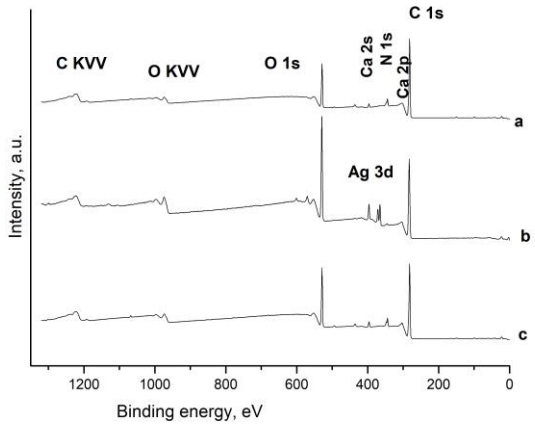

Fig. 3. XPS survey spectra for Ag/Chit (a), Ag/ChitFilm (b) and ChitFilm (c), the spectra are normalized by intensity of the C 1s peak.

According to Fig. 3 the survey spectrum of Ag/ChitFilm does not contain signals from silver atoms while other methods confirm the presence of silver in the film. Given the information depth of the XPS method, it can be assumed that the metal is not in the near-surface region and when the metal-containing composite is formed, the silver nanoparticles encapsulate into the deeper layers of the composite (more than 10 nm). The C 1s, N 1s and O 1s core-shell photoelectron spectra for all composites are presented in Fig. 4.

Table 2. Surface elemental composition (% at.) of the samples obtained from the survey spectra.

Element	Ag/Chit	Ag/ChitFilm	ChitFilm
O	27.9	16.3	20.6
N	6.0	2.0	2.8
C	65.0	79.5	74.3
Ag	1.1	-	-
Si	-	0.59	0.42
Ca	-	1.5	1.6
Na	-	0.1	0.3

Fig. 5 shows the C 1s photoelectron spectra charge referenced to the binding energy of 288.2 eV related to O-C-O group of chitosan. It should be noted that according to the literature data the C 1s spectrum of chitosan is often described with two main states with binding energies of 286.0-286.5 and 288.0-288.5 eV which are attributed to carbon atoms in ***C***-N/***C***-O/***C***-O-***C*** and ***C***(O)N/C(O)O functional groups [17-20]. In this work, the more reliable fitting procedure has been used. The C 1s spectrum of Ag/Chit composite was fitted with peaks at 285.8, 286.7, 288.1 and 288.9 eV which can be assigned to ***C***-N, ***C***-O/***C***-O-***C***, O-***C***-O, ***C***(O)N functional groups (amino, hydroxyl/ether, glycosidic and amide groups). Peak at binding energy of 285.0 eV is no characteristic for the chitosan structure and assigned to the adventitious carbon. The chemical structure of chitosan molecule was taken into account within the curve fitting procedure; specifically the relative intensities of the signals with binding energies of 285.8, 286.5 and 288.1 eV were used as 1:4:1. This intensity ratio was applied within the spectra analysis of other samples as much as possible.

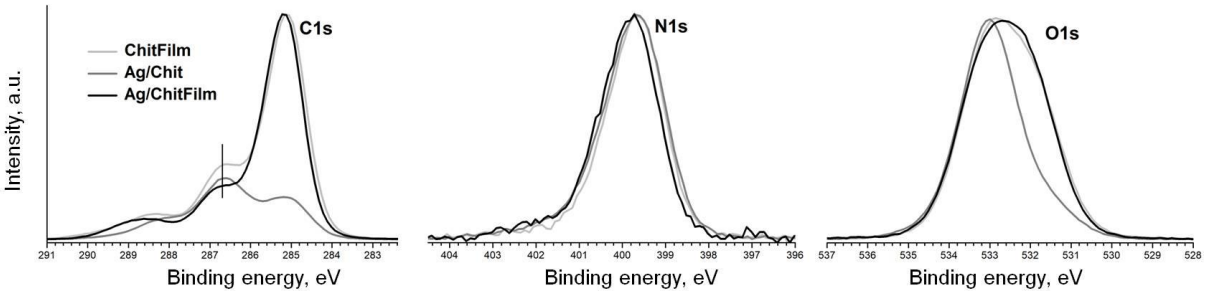

Fig. 4. C 1s, N 1s and O 1s core-shell photoelectron spectra for ChitFilm, Ag/ChitFilm and Ag/Chit composites.

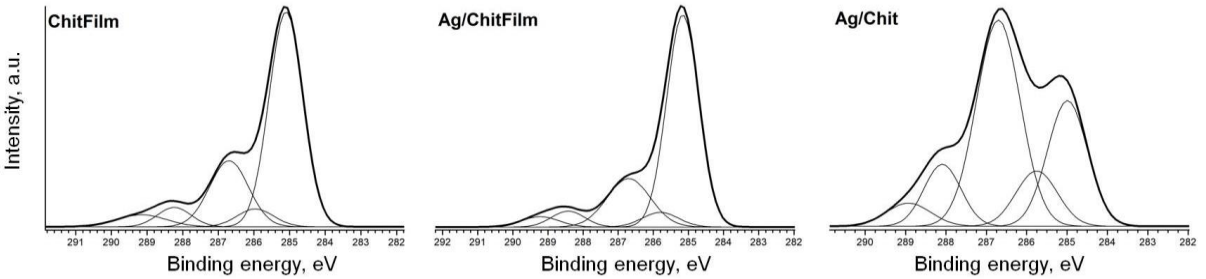

Fig. 5. High-resolution photoelectron C 1s spectra for the composites and their fitting with five components.

Data on the relative concentrations of carbon-containing chemical groups (at.%) obtained from fitting the high-resolution C 1s spectra are shown in Table 3. The concentration of adventitious ***C***-C/***C***-H carbon in ChitFilm and Ag/ChitFilm composite is significantly higher than that of the Ag/Chit composite, it may be explained by the presence of acetic acid in them.

Table 3. Quantity analysis of the surface chemical composition of the samples based on photoelectron C 1s spectra.

		Group				
Sample		***C***-C/***C***-H	***C***-N	***C***-O/***C***-O-C	O-***C***-O	***C***(O)N/ ***C***(O)O
ChitFilm	E	285.1	286.0	286.7	288.2	289.2
	W	0.95	1.02	1.10	0.94	1.38
	at.%	**62**	**6**	**22**	**6**	**5**
Ag/ChitFilm	E	285.2	285.8	286.7	288.4	289.2
	W	0.91	1.02	1.24	0.94	1.06
	at.%	**66**	**5**	**20**	**5**	**4**
Ag/Chit	E	285.0	285.8	286.7	288.1	288.9
	W	0.99	1.02	1.10	0.91	1.10
	at.%	**25**	**12**	**46**	**12**	**5**

Fitting the N 1s spectra with three components (Fig. 6) reveals that the chitosan-based composites contain peaks which can be assigned to nitrogen atoms in the functional groups of ***N***-C , ***N***(O)C and $^{+}$***N***-C (non-protonated amino, amid and protonated amino groups). According to the previous works the N 1s spectra of chitosan-based materials often have two main contributors to the N 1s spectra: at ca. 399.3 eV due to non-protonated amine and amide as well as small peak at ca. 401.3 eV attributed to the protonated amine [21].

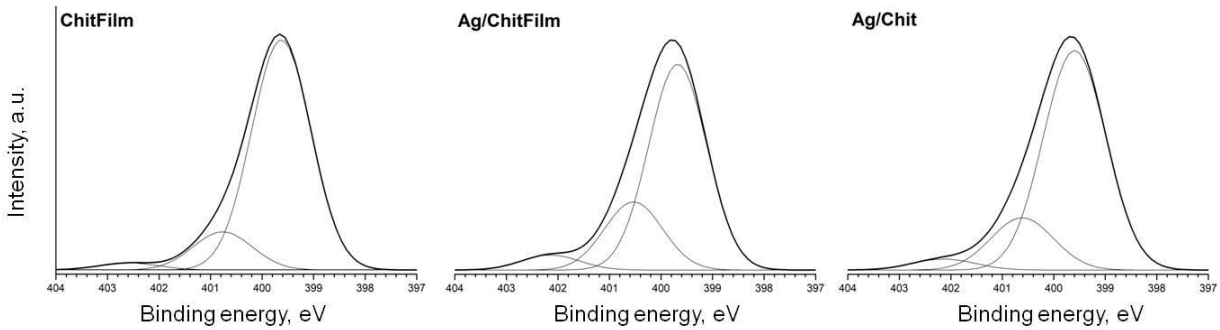

Fig. 6. High-resolution photoelectron N 1s spectra for the composites and their fitting with three components.

Data on the relative concentrations of nitrogen-containing chemical groups (at.%) obtained from the fitting the N 1s high-resolution spectra are shown in Table 4. The N 1s peaks broadening of Ag/Chit may indirectly indicate both the heterogeneity of the sample surface and the appearance of a new state associated with the interaction of silver particle with chitosan.

Table 4. Quantity analysis of the surface chemical composition of the samples based on photoelectron N 1s spectra.

		N 1s		
Sample		***N***-C	***N***(O)C	$^{+}$***N***-C
ChitFilm	E	399.6	400.8	402.1
	W	1.15	1.15	1.15
	at.%	**84**	**14**	**3**
Ag/ChitFilm	E	399.7	400.5	402.1
	W	1.13	1.13	1.13
	at.%	**71**	**24**	**5**
Ag/Chit	E	399.6	400.6	402.1
	W	1.22	1.22	1.22
	at.%	**78**	**18**	**4**

According to fitting the high-resolution N 1s spectra relative concentration of protonated and non-protonated groups for the Ag/ChitFilm is about 1:14 (5:71) while for the Ag/Chit and ChitFilm composites this ratio is about 1:19 (4:78) and 1:28 (3:84), respectively. Calculated ratio of concentration of non-protonated amino to amide group are 6:1 (84:14), 4.3:1 (78:18), 3:1 (71:24) for ChitFilm, Ag/Chit and Ag/ChitFilm, respectively.

It can be assumed that the decrease in concentration of amino groups and the increase in concentration of amide groups on the surface in the aforementioned samples sequence may indicate possible interaction of amino groups of chitosan with silver nanoparticles, and as a consequence the special arrangement of chitosan macromolecules during the film formation.

Fig. 7 shows the photoelectron Ag 3d and Ag $M_{45}N_{45}N_{45}$ Auger spectra for the Ag/Chit composite. The photoelectron peaks of Ag $3d_{5/2}$ and Ag $3d_{3/2}$ are registered at binding energies of 368.5 and 374.5 eV, respectively. These binding energies are characteristic of silver atoms in zero-valent state [22, 23]. The kinetic energy of the Ag $M_{45}N_{45}N_{45}$ is 357.4 eV.

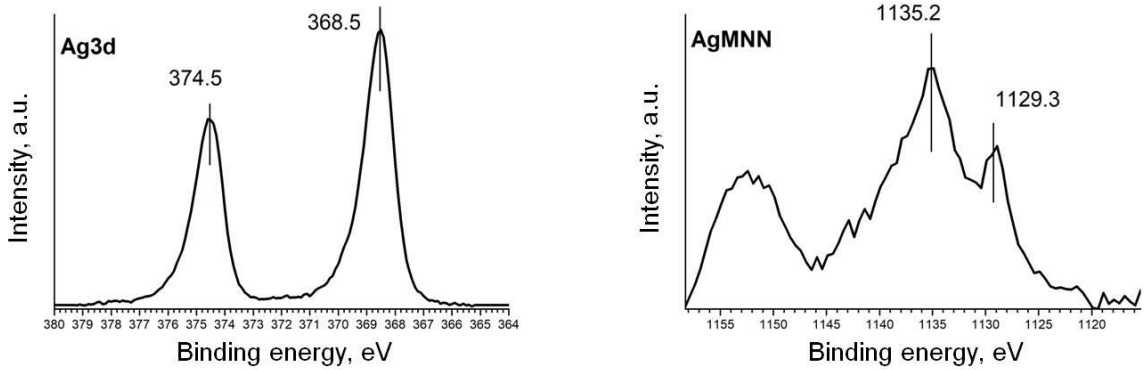

Fig. 7. High-resolution photoelectron Ag 3d (on the left) and Ag MNN Auger (on the right) spectra for Ag/Chit composite.

The Auger parameter calculated as the sum of the Ag $3d_{5/2}$ binding energy and Ag $M_{45}N_{45}N_{45}$ kinetic energy is 725.9. The value indicates that silver on the surface of the Ag/Chit composite is in a non oxidized state [22].

4. CONCLUSIONS

In this work the novel route for preparing chitosan films with silver nanoparticles using MVS is proposed. ATR-FTIR analysis showed that spectra of the modified with silver nanoparticles and nonmodified chitosan-based films are rather similar. However, the significant decrease in absorbance of all bands is detected. Furthermore, detailed analysis of amide I and amide II regions with deconvolution procedure revealed the changes in the relative intensities of the bands. The detected spectral features may be related to the electrostatic interaction of chitosan groups with silver nanoparticles. The surface composition of the films was determined by means of XPS analysis. The changes in the concentration of nitrogen containing groups indicate possible interaction of amino groups of chitosan with silver nanoparticles and as a consequence the special arrangement of chitosan macromolecules during the film formation.

ACKNOWLEDGEMENTS

This work was supported by Russian Foundation for Basic Research grant №18-33-01094. The authors gratefully acknowledge Center for molecule composition studies (INEOS RAS), Center for Collective Use (MSU), Dr. S.V. Savilov and Dr. K.I. Maslakov for recording the XPS spectra and Dr. S.S. Abramchuk for TEM measurements.

REFERENCES

[1] M. Rinaudo, *Chitin and Chitosan: Properties and applications*, Progress in Polymer Science, 31 (2006) 603-632.

[2] L.A.M. van den Broek, R.J.I. Knoop, F.H.J. Kappen, C.G. Boeriu, *Chitosan films and blends for packaging material*, Carbohydrate Polymers (2014), doi: 10.1016/j.carbpol.2014.07.039.

[3] G. Cárdenas, J. Díaz, M. F. Meléndrez, C. Cruzat, *Physicochemical properties of edible films from chitosan composites obtained by microwave heating*, Polymer Bulletin 61 (2008) 737-748.

[4] M. L. Ojeda-martínez, I. Yáñez-sánchez, C.Velásquez-ordoñez, M. M. Martínez-palomar, A. Álvarez-rodríguez, M. A Garcia-sánchez, F. Rojas-gonzález, F. J Gálvez-gastélum, *Skin wound healing with chitosan thin films containing supported silver nanospheres*, Journal of Bioactive and Compatible Polymers 30 (2015) 1-16.

[5] M. K. Rai, S. D. Deshmukh, A. P. Ingle, A. K. Gade, *Silver nanoparticles: The powerful nanoweapon against multidrug-resistant bacteria*, Journal of Applied Microbiology 112 (2012) 841-852.

[6] S.H. Ding, W.P. Qian, Y. Tan, Y. Wang, *In-Situ Incorporation of Gold Nanoparticles of Desired Sizes into Three-Dimensional Macroporous Matrixes*, Langmuir 22 (2006) 7105-7108.

[7] D. Wei, W. Qian, *Facile synthesis of Ag and Au nanoparticles utilizing chitosan as a mediator agent*, Colloids and Surfaces B: Biointerfaces 62 (2008) 136-142.

[8] M.A. Moharram, S.K.H. Khalil, H.H.A. Sherif, W.A. Khalil, *Spectroscopic study of the experimental parameters controlling the structural properties of chitosan-Ag nanoparticles composite*, Spectrochimica Acta Part A: Molecular and Biomolecular Spectroscopy 126 (2014) 1-6.

[9] M.S. Rubina, E.E. Kamitov, Y.V. Zubavichus, G.S. Peters, A.V. Naumkin, S. Suzer, A.Yu. Vasil'kov, *Collagen-chitosan scaffold modifying with Au and Ag nanoparticles: synthesis, structure and properties*, Applied Surface Science 366 (2016) 365-371.

[10] A.B. Smetana, K.J. Klabunde, G.R. Marchin, C.M. Sorensen, *Biocidal Activity of Nanocrystalline Silver Powders and Particles*, Langmuir 2008 (24) 7457-7464.

[11] G. Cárdenas-Triviño, M. Ruiz-Parra, L. Vergara-González, J. Ojeda-Oyarzún, G. Solorzano, *Synthesis and Bactericidal Properties of Hyaluronic Acid Doped with Metal Nanoparticles*, Journal of Nanomaterials 2017 (2017) 1-9.

[12] A.Yu. Vasil´kov, M.S. Rubina, A.V. Naumkin, Ya. V. Zubavichus, O. A. Belyakova, Yu. V. Maximov, V.K. Imshennik, *Metal-containing system based on chitosan and a collagen-chitosan composite*, Russian Chemical Bulletin 64 (2015) 1663-1670.

[13] M.S. Rubina, A.Yu. Vasil´kov, A.V. Naumkin, E.V. Shtykova, S. S. Abramchuk, M. A. Alghuthaymi, K.A. Abd-Elsalam, *Synthesis and characterization of chitosan-cooper nanocomposites and their fungicidal activity against two sclerotia-forming plant pathogenic fungi*, Journal of Nanostructure Chemistry 7 (2017) 249-258.

[14] K.A. Abd-Elsalam, A.Yu. Vasil´kov, E.E. Said-Galiev, M.S. Rubina, A.R. Khokhlov, A. V. Naumkin, E.V. Shtykova, M.A. Alghuthaymi. *Bimetallic blends and chitosan nanocomposites: novel antifungal agents against cotton seedling damping-off*, European Journal of Plant Pathology 151 (2018) 57-72.

[15] C. Paluszkiewicz, E. Stodolak, M. Hasik, M. Blazewicz, *FT-IR study of montmorillonite-chitosan nanocomposite materials*, Spectrochimica Acta Part A: Molecular and Biomolecular Spectroscopy 79 (2011) 784-788.

[16] J. Díaz-Visurraga, C.Daza, C. Pozo, A. Becerra, C. von Plessing, A. García, *Study on antibacterial alginate-stabilized copper nanoparticles by FT-IR and 2D-IR correlation spectroscopy*, International Journal of Nanomedicine 7 (2012) 3597-3612.

[17] H. Maachou, M. J. Genet, D. Aliouche, C. C. Dupont-Gillain and Paul G. Rouxhet, *XPS analysis of chitosan–hydroxyapatite biomaterials: from elements to compounds*, Surface Interface Analysis 45 (2013) 1088–1097.

[18] P. G. Rouxhet, M. J. Genet, *XPS analysis of bio-organic systems*, Surface Interface Analysis 43 (2011) 1453-1470.

[19] J.M. Vaz, T.B. Taketa, J. Hernandez-Montelongo, P. Chevallier, M.A. Cotta, D. Mantovani, M.M. Beppu, *Antibacterial properties of chitosan-based coatings are affected by spacer-length and molecular weight*, Applied Surface Science (2018), doi: 10.1016/j.apsusc.2018.03.110.

[20] B. Jurado-López, R.S. Vieira, R.B. Rabelo, M.M. Beppu, J. Casado, E. Rodríguez-Castellón, *Formation of complexes between functionalized chitosan membranes and copper: A study by angle resolved XPS*, Materials Chemistry and Physics (2016), doi: 10.1016/ j.matchemphys.2016.10.018.

[21] A. P. Carapeto, A. M. Ferraria, A. M. Botelho do Rego, *Unraveling the reaction mechanism of silver ions reduction by chitosan from so far neglected spectroscopic features*, Carbohydrate Polymers 174 (2017) 601–609.

[22] S.W. Gaarenstroom., Winograd N. J., *Initial and final state effects in the ESCA spectra of cadmium and silver oxides*, The Journal of Chemical Physics 67(1977) 3500-3506.

[23] V.Y. Young, R. A. Gibbs, N. J. Winograd, *X-ray photoemission studies of atom implanted matrices: Cu, Ag, and Au in SiO_2*. The Journal of Chemical Physics, 70 (1979) 5714-5721.